

PROCEEDINGS OF SPIE

[SPIDigitalLibrary.org/conference-proceedings-of-spie](https://spiedigitallibrary.org/conference-proceedings-of-spie)

Intraoperative imaging using intravascular contrast agent

Jeffrey R. Watson
Nikolay Martirosyan
Summer Garland
G. Michael Lemole
Marek Romanowski

SPIE.

Intraoperative Imaging using Intravascular Contrast Agent

Jeffrey R Watson^{a*}, Nikolay Martirosyan^b, Summer Garland^a, G Michael Lemole Jr^b, Marek Romanowski^a

^aDept of Biomedical Engineering, University of Arizona, 1657 E Helen St, Tucson, AZ, 85721;

^bDept. of Neurosurgery, Division of Surgery, Banner University Medical Center, Tucson Campus, 1501 N Campbell Ave, Tucson, AZ 85724

*marekrom@email.arizona.edu; phone 1 520 626-2578; fax 1 520 626-4824; bme.arizona.edu

ABSTRACT

Near-infrared contrast agents are becoming more frequently studied due to their advantageous characteristics, most notably the ability to work in the tissue transparency window of the electromagnetic spectrum. This produces a need for imaging technology that can be specific for both the NIR dye and the discipline. Indocyanine green is currently the primary NIR dye used in neurosurgery. Here we report on using the previously described augmented microscope for image guidance in a rat glioma resection. Luc-C6 cells were implanted in a rat in the left-frontal lobe and grown for 22 days. Surgical resection was performed by a neurosurgeon using augmented microscopy guidance with ICG contrast. Videos and images were acquired to evaluate image quality and resection margins. ICG accumulated in the tumor tissue due to enhanced permeation and retention from the compromised blood-brain-barrier. The augmented microscope was capable of guiding the rat glioma resection and highlighted tumor tissue regions via ICG signal.

Keywords:

1. INTRODUCTION

There were an estimated 22,850 new brain tumor cases in the US in 2015 as reported by the NIH SEER. Although not a large number compared to total cancers, the 5-year survival rate of this particularly insidious cancer remains around 30%. The American Brain Tumor Association indicates the prognosis decreases significantly when staged as an anaplastic astrocytoma where median survival is 2-3 years, and more aggressive glioblastoma multiforme (GBM) can decrease median survival to less than 14 months. Surgery is typically the primary treatment for these tumors followed by adjunct chemotherapy and radiotherapy. However, GBM is known for its invasive growth, quickly infiltrating normal tissue of the brain. Therefore, it is often difficult to visualize tumor margins and achieve complete tumor resection. As the development of invasive GBM is accompanied by the growth of abnormal vascular network that feeds the tumor, vascular angiography has become a valuable tool for improved visualization of tumor margins and surgical resection.

Fluorescence imaging has seen considerable advances over the past decade including the more recent investigation and clinical applications of near-infrared fluorescence imaging (NIRF).¹ Many researchers have developed new imaging devices for specific near-infrared (NIR) fluorescence applications.²⁻⁵ While indocyanine green (ICG) is not a tumor-selective probe, the compromised blood-brain-barrier caused by the invasive glioma allows for increased enhanced permeation and retention (EPR) of the dye in the regions of tumors. Indeed, ICG has been shown to accumulate in astrocytoma grown in mice and imaged using a confocal endomicroscope.⁶ Subsequently, there has been increased use of ICG dye to evaluate blood flow and vascular anomalies in cerebrovascular surgeries.⁷

2. MATERIALS AND METHODS

2.1 C6 cell transduction

All animal procedures were approved by the University of Arizona Institutional Animal Care and Use Committee.

Rat glioma C6 cell line was purchased from ATCC. The cells were treated with a lentiviral vector (Cignal Lenti Positive Control (luc), Qiagen, Valencia, CA) to transduce the cells with luciferase gene using a puromycin selector (Santa Cruz

Biotechnology, Dallas, TX) and a transducing reagent to enhance transduction efficiency. Luminescence was confirmed using a plate reader.

2.2 Cell implantation

We used 200 g adult female Wistar rats (n=4). The rats were anesthetized by intraperitoneal injection of a ketamine/xylazine cocktail (80mg/kg, 12mg/kg) prepared at a dose of 1 mL/kg. Presurgical injections of saline and gentamycin (8mg/kg) were given for hydration and antibiotics respectively. The rats were placed into a stereotactic frame for cell implantation. Coordinates for cell implantation were 1 mm A/P, 3.5 mm M/L, 3.5 mm V/D measured from bregma. We injected 10^5 luc-C6 cells suspended in 5 μ L volume at a rate of 1 μ L per minute with a 10 μ L Hamilton syringe and a 28 gauge cannula (Plastics One, Roanoke, VA). The cannula was slowly advanced ventrally 4 mm and then retracted 0.5 mm after 1 minute to create a pocket for cell infusion. Following cell infusion, 1 minute elapsed before the cannula was retracted out of injection site. The access hole was closed with bone wax and the scalp closed using wound clips. The tumor was grown in the rat for 22 days. Tumor growth was followed using bioluminescence imaging (BLI) system (LagoX, Tucson, AZ) with luciferin and magnetic resonance imaging (MRI) (BioSpec 7T, Bruker, Billerica, MA). We performed T1 weighted imaging with 150 μ L injection of 0.5 M gadolinium contrast (Multihance, Bracco Diagnostics, Cranbury Township, NJ) to enhance visualization of the tumor. This is consistent with current clinical practice to confirm tumor growth in the clinic. The size of the tumor for resection was confirmed using MRI within 24 hours of resection.

2.3 Glioma resection

Tumor resection was performed by a neurosurgeon at the Banner University Medical Center, Tucson Campus. Following a full craniotomy and prior to tumor resection, each rat was injected with luciferin and imaged in the BLI system pre- and post-surgery. Resection was performed under standard microscopy (n=2) and augmented microscopy with ICG (n=2). ICG was injected 15 minutes prior to resection under augmented microscopy guidance. Video of all resection procedures were recorded. Representative snapshots of the videos are shown in Figure 5.

All BLI imaging was performed with 8-bit dynamic range and a 10-minute exposure time. Rats were injected with 0.4 mL of luciferin prepared at 50 mg/mL (GoldBio, Olivette, MO). Dose of luciferin was prepared according to the protocol supplied by GoldBio. Rats were anesthetized for BLI imaging using 1-3% isoflurane. Percent tumor growth was calculated by drawing a region of interest around the luminescence boundary in BLI images and integrating the intensity values. Duration of the surgical procedure did not exceed 30 minutes. No additional luciferin injection was given post-surgery with the assumption that continued luminescence from the remaining and resected tumor tissue would still be present. After tumor resection and post-surgical BLI imaging, the brain was explanted and placed in paraformaldehyde. Resected tumor tissue was placed in freezing solution and flash frozen in liquid nitrogen. All samples were prepared for histology. ICG dose was calculated according to standard clinical dose (Akorn Pharmaceuticals, Lake Forest, IL) and scaled by body weight for rat injection. The rats used for resection with augmented microscopy guidance were injected with 1 mL of 62.5 μ g/mL solution of ICG (Sigma-Aldrich, St. Louis, MO) to yield a dose of 25mg/80kg.

3. RESULTS

Tumor growth was monitored using BLI. Figure 1 shows a representative time lapse of tumor growth in one of the rats over 5 imaging time points plus the post-resection time point. A plot of tumor growth over time is shown in Figure 2. Also represented in both Figure 1 is the resection time point (day 22). We saw an exponential growth of the tumor (Figure 2).

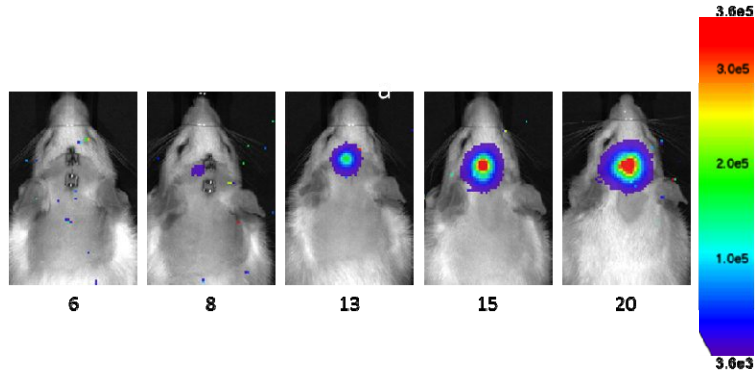


Figure 1: BLI imaging of luc-C6 glioma growth in a rat over 20 days (68R2).

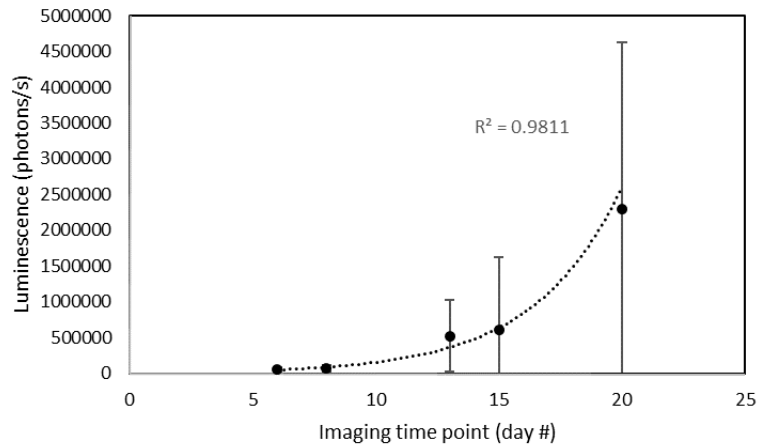


Figure 2: Tumor growth followed using BLI imaging. Tumor growth determined by integration of luminescence intensity on the BLI system (68R2).

T1 weighted MRI with gadolinium contrast was used to confirm tumor growth in the animals on day 22 (Figure 3). These images were supplied to the neurosurgeon preoperatively for surgical planning.

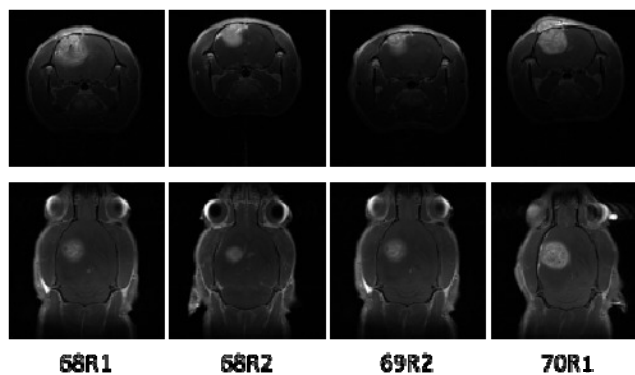


Figure 3: T1 weighted MRI with gadolinium contrast showing tumor growth in the rat brain. Images were captured at day 22 (within 24 hours of resection). Transverse and horizontal slices are shown on top and bottom respectively. All slices are at the same depth for transverse and horizontal slices respectively.

As seen in Figure 1, there is an apparent drop in luminescence signal after surgery due to the reduced luminescence from tumor cells that were resected. However, it is also apparent that after resection, there is still the presence of tumor cells in the resection bed. This is consistent across all animals (Figure 4). The neurosurgeon collected a majority of the

resected tissue on a sample dish that was imaged with BLI beside the exposed resection bed in the animal. The threshold scale between Figures 1 and 4 was adjusted to account for luminescence intensity changes following craniotomy. The threshold was adjusted to optimize luminescence boundary and minimize noise.

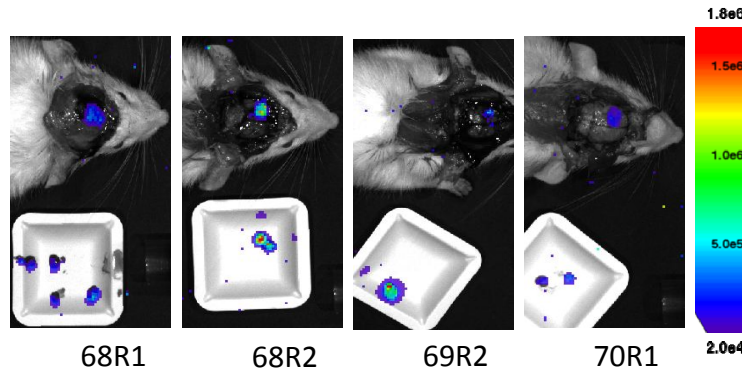


Figure 4: Post-resection BLI showing the exposed resection bed and the resected tumor tissue in a sample dish beside the animal.

Tumor resection was performed under both standard bright-field microscopy, similar to current practice in the clinic, and under augmented microscopy with ICG contrast. Figure 5 shows an example of accumulation of ICG in the tumor tissue. It is apparent in Figure 5d, the green signal, that some tumor tissue was left behind. This is consistent with post-resection BLI imaging showing remaining tumor tissue.

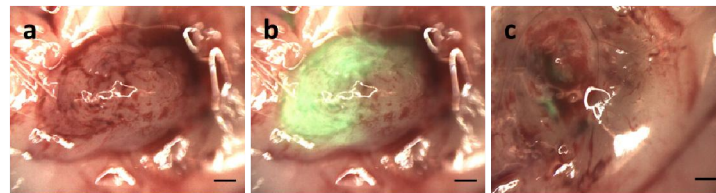


Figure 5: Brain tumor in a rat (70R1). Pre-resection images (a) visible, (b) augmented pre-resection, and (c) augmented post-resection. Scale bar equals 1 mm.

Standard hematoxylin and eosin (H&E) staining was performed on 6 μ m sections taken from the resection bed of the rat brains. Figure 6 shows a representative section of the brain tissues. The 2x magnification images shows the resection bed and the subsequent magnifications show the clear and distinct margin of cancerous versus normal tissue. Histology appears consistent with tumor cells left in the resection bed as shown in the BLI images above and in the representative augmented microscopy images.

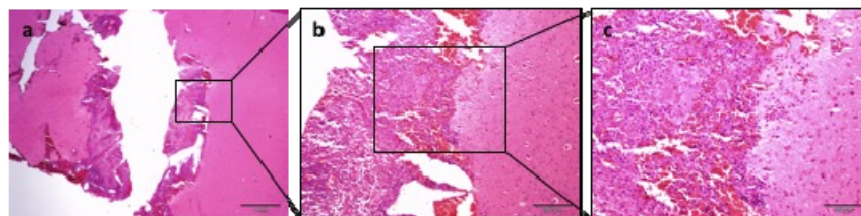


Figure 6: Hematoxylin and eosin stain on representative slice of brain at resection bed. (a) 2x magnification, (b) 10x magnification, and (c) 20x magnification. Scale bars are 1 mm, 200 μ m, and 100 μ m respectively (69R2).

4. CONCLUSIONS

Current clinical practice requires the surgeon to visualize the visible and NIR images independently, whereas the augmented microscope presents these images superimposed and in real-time for more accurate registration between the images. The augmented microscope produced these images with excellent contrast to the bright-field image and was able to minimize throughput of NIR noise to the augmented image with only simple thresholding. This limits processing time thereby reducing any lag in the real-time image processing and display. The extent of resection was at the discretion of the neurosurgeon and the augmented microscope was only used for improved image guidance and not in an effort to

change the neurosurgeon's resection decision(s). ICG was injected intravenously. The dye is quickly cleared from the circulation with atypical half-life of 3 minutes. As visualized under the augmented microscope, the dye showed apparent diffusion and retention into tumor tissue, likely due to a compromised blood-brain-barrier caused by the invasive glioma. Post-resection BLI imaging showed remanence of tumor cells even after using the augmented microscope for image guidance. We suggest that this is due the non-specific nature of ICG distribution in the tumor and that the fluorescent molecule did not penetrate through the entire tumor margin. Therefore, it is probable that tumor cells extend beyond the boundary delineated by ICG signal.

Notably, we demonstrated that tumor growth in the rat can be monitored non-invasively by BLI through the intact skull and scalp. In comparison, post-resection BLI (Figure 4) was performed in situ with neither the skull nor scalp were present. However, with different experimental condition, the threshold values and luminescence signal scales are different between Figure 1 and 4.

It is evident in Figure 5b that the luminescence appears to have a gradient over the tumor tissue. This is likely a consequence from the non-stereoscopic configuration of the augmentation channel and produces an uneven illumination field and/or detection. Again, this is due to excitation and detection being performed in only one optical path.⁵ Future development aims to move to a fully stereoscopic configuration thereby eliminating this gradient effect.

The development of augmented microscopy has proven to provide a unique imaging environment for oncologic surgical procedures. With the continued development of novel NIR contrast agents, the augmented microscope aims to visualize such fluorophores and to guide surgical procedures or therapies. Future work will aim to involve molecular targeting fluorophores and ultrafast laser surgery, both applications that can be visualized and guided under the augmented microscope.

5. ACKNOWLEDGEMENTS

This work was supported by NIH grant HL007955. MR and GML acknowledge support of the Harrison H. and Catherine C. Barrett Imaging Grant and the University of Arizona TRIF Optics/Imaging Program. JRW acknowledges support from the ARCS Foundation Crawford family donation. The authors acknowledge Dr. Theodore P. Trouard and Michael Valdez for their assistance in MRI experiments.

REFERENCES

- [1] Sevick-Muraca, E. M., "Translation of near-infrared fluorescence imaging technologies: emerging clinical applications," *Annu Rev Med* 63, 217-231 (2012).
- [2] Marshal, M. V., Rasmussen, J. C., Tan, I-C., Aldrich, M. B., Adams, K. E., Wang, X., Fife, C. E., Maus, E. A., Smith, L. A., Sevick-Muraca, E. M., "Near-infrared fluorescence imaging in humans with indocyanine green: a review and update," *Open Surg. Oncol. J.* 2(2), 12-25 (2010).
- [3] Elliott, J. T., Dsouze, A. V., Davis, S. C., Olson, J. D., Paulsen, K. D., Roberts, D. W., Pogue, B. W., "Review of fluorescence guided surgery visualization and overlay techniques," *Biomed. Opt. Express* 6(10), 3765-3782 (2015).
- [4] Frangioni, J. V., "In vivo near-infrared fluorescence imaging," *Curr. Opin. Chem. Biol.* 7(5), 626-634 (2003).
- [5] Watson, J. R., Gainer, C. F., Martirosyan, N., Skoch, J., Lemole, G. M., Anton, R., Romanowski, M., "Augmented microscopy: real-time overlay of bright-field and near-infrared fluorescence images," *J. Biomed. Opt.* 20(10), 106002 (2015).
- [6] Martirosyan, N. L., Cavalcanti, D. D., Eschbacher, J. M., Delaney, P. M., Scheck, A. C., Abdelwahab, M. G., Nakaji, P., Spetzler, R. F., Preul, M. C., "Use of in vivo near-infrared laser confocal endomicroscopy with indocyanine green to detect the boundary of infiltrative tumor," *J. Neurosurg.* 115(6), 1131-1138 (2011).
- [7] Raabe, A., Nakaji, P., Beck, J., Kim, L. J., Hsu, F. P., Kamerman, J. D., Seifert, V., Spetzler, R. F., "Prospective evaluation of surgical microscope-integrated intraoperative near-infrared indocyanine green videoangiography during aneurysm surgery," *J. Neurosurg.* 103(6), 982-989 (2005).